

HARNESSING TITANIUM DIOXIDE SURFACE TOWARD NOVEL FUNCTIONAL MATERIALS

José A. Solera-Rojas^{1,2}, Christin K. Rapp^{2†}, M. Cinthya Rivera-Martínez^{1,2†}, Leslie W. Pineda^{1,2*}

¹School of Chemistry, University of Costa Rica 11501-2060 San Jose, Costa Rica.

²Center of Electrochemistry and Chemical Energy (CELEQ), University of Costa Rica, 2060 San Jose, Costa Rica.

[†]Current address: Technische Universität München, Munich, Germany.

[†]Current address: Celco de Costa Rica S. A., Cartago, Costa Rica.

Recibido julio 2015; Aceptado diciembre 2015

Abstract

The ever-increasing worldwide energy consumption has led the society to quest for novel and functional materials that can be used in the development of solar fuels to some extent lessen the dependence on fossil fuels. In this context, the role of titanium dioxide has been investigated to generate versatile materials able to harness the light emitted by the Sun. Thus, the main research avenues of such semiconductor oxide are focus on dye-sensitized solar cells (DSSCs) and photoelectrochemical cells for the oxidation of water molecule. Indeed, the modification of the semiconductor oxide surface by band-gap engineering greatly enhances its optical properties and catalytic activity. In this review, we address some fundamental issues regarding structural, optical and electronic properties that render TiO₂ a versatile substrate in surface chemistry, and as entry for anchoring and functionalization strategies for the development of solar cell devices and catalytically active surfaces.

Resumen

El alto consumo de energía a nivel mundial ha llevado a la búsqueda de nuevos materiales que puedan utilizarse en el desarrollo de los combustibles solares, y así disminuir la dependencia hacia los derivados del petróleo. Debido a esto, por mucho tiempo se ha investigado el papel del dióxido de titanio para generar nuevos materiales capaces de aprovechar la luz emitida por el Sol. Dos ejes centrales en la investigación del TiO₂ son el uso en celdas solares sensibilizadas con tintes (DSSC) y celdas fotoelectroquímicas para la oxidación de la molécula de agua, en donde uno de los principios básicos es la modificación de las propiedades ópticas del TiO₂ para mejorar su actividad. Por tanto, en este artículo de revisión de la literatura se discutirán las características estructurales, ópticas y electrónicas del TiO₂, así como la modificación en superficie para el desarrollo de dispositivos en celdas solares y superficies catalíticamente activas.

Key words: Titanium dioxide, dye-sensitized solar cells, photoelectrochemical cells, water-oxidation reaction, solar fuels, surface modification.

Palabras clave: Dióxido de titanio, celdas solares sensibilizadas con tintes, celdas fotoelectroquímicas, reacción oxidación del agua, combustibles solares, modificación de superficie.

I. INTRODUCTION

Titanium is the ninth most abundant metal in Earth crust (ca. 0.6%). It is found in nature in the mineral form of ilmenite (FeTiO₃), with three main forms of titanium dioxide (TiO₂) (i.e.,

* Corresponding author: leslie.pineda@ucr.ac.cr

anatase, rutile and brookite) and perovskite (CaTiO_3). Only about 5% of annually world production goes to the manufacture of titanium metal; the other 95% corresponds to the production of TiO_2 [1].

The annual world consumption of TiO_2 reaches up to 3 million tons, being its major use as a pigment, due to a high refractive index, easiness to prepare particles of small sizes with a great superficial area and light-scattering ability, and its whiteness [2-3]. Other applications include sunscreen [4], skincare products [5], toothpaste [6], food additive [7], semiconductors [8], and more recent as photocatalyst for the oxidation reaction of water [9-15].

As to TiO_2 polymorphs, rutile is the only stable phase, while anatase and brookite are metastable phases and can be converted to rutile irreversibly by heating. These forms have different crystal structures, being all of them distorted octahedra. The brookite polymorph crystallizes as an orthorhombic crystal system; rutile forms a distorted tetragonal system, and anatase a tetragonal crystal system [16-17]. (Fig. 1)

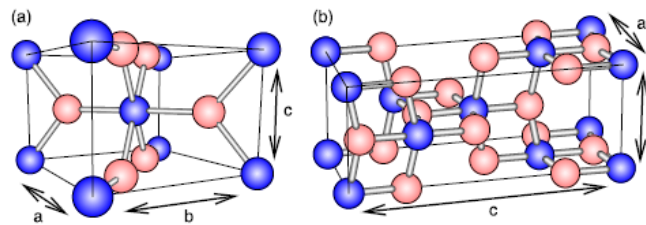


FIGURE 1. Schematic representation of the unit cell for the polymorphs of TiO_2 , (a) rutile $a = b = 4.49 \text{ \AA}$; $c = 3.01 \text{ \AA}$; and (b) anatase $a = b = 3.77 \text{ \AA}$; $c = 9.56 \text{ \AA}$. Ti^{4+} ions are in blue and O^{2-} ions are in red. From [18], reproduced with permission.

Recently, it has been found new physical and chemical properties concerning the size of the material. Depending on the preparation method, one can generate nanoparticles, nanotubes, nanowires, etc. Such protocols include sol-gel, micelle and inverse micelle, hydrothermal, solvothermal, direct oxidation, chemical and physical vapor deposition, electrodeposition, sonochemical, microwaves, etc, reviewed elsewhere. [19-20]

Then, the applications of TiO_2 nanomaterials greatly rely on their optical properties, so currently there is a great body of fundamental and applied research in the modification of the surface oxide with organic and inorganic molecules to improve the optical sensitivity and activity in the ultraviolet and visible region of the electromagnetic spectrum. In this review, we highlight the structural, thermodynamic, electronic and optical properties of TiO_2 , and the surface modifications that can be made to enhance their efficiency, either for solar cells devices or photocatalysis.

II. PROPERTIES OF TITANIUM DIOXIDE

Structural properties

Rutile and anatase are the two most important crystalline structures of TiO_2 . (Fig. 1) Both can be described as octahedral chains of TiO_6 , where each Ti^{4+} ion is surrounded by six O^{2-} ions, in

an octahedral fashion. The difference between these crystal structures resides in the distortion of the octahedral and mounting pattern of the octahedral chains. In the rutile phase, the octahedral array shows a slight orthorhombic distortion with O^{2-} ions in a hexagonal close-packed lattice (hcp) and half of the octahedral holes occupied by centers of Ti(IV); while in the anatase phase, the octahedron is significantly distorted, so that the symmetry is smaller than the orthorhombic with O^{2-} ions in a cubic close-packed lattice (ccp). The bond distance Ti–Ti in anatase is bigger than rutile, while Ti–O bond lengths are shorter. [19] These features in the structure packing cause differences in bulk densities and electronic band structures of TiO_2 .

Several studies have shown that the metastability of anatase is functioning of the pressure and dependent of the size, since the smaller the crystals; the structure is preserved at higher pressures. For example, three metastable phases can be attained synthetically by induced pressure for transition phases to ambient temperature: anatase to amorphous which are crystals of small size, the transition anatase to baddeleyite that are crystals of intermediate size and anatase to PbO_2 -like, when comprising nanocrystals to macroscopic crystals. [3,21]

Titanium dioxide surface

The crystal structure of the surface affects the chemical reactions and photoactivity that can be carried out on surface itself. Each crystal plane has different content of titanium and various sites of oxygen atoms. [11] It is important to note the crystal facets in which the process occur to describe the adsorption and coordination in the TiO_2 surface, for instance, the adsorbate/metallic-oxide interaction always refers to a specific crystallographic plane. Thus, the more stable and characterized crystal facets are (101) for anatase and (110) for rutile [11], as shown in Fig. 2.

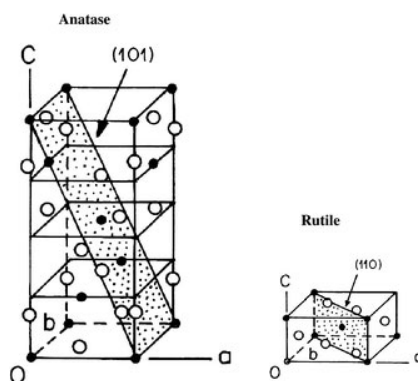


FIGURE 2. Units cells of anatase and rutile showing the (101) and (110) crystallographic planes, respectively. From [22], reproduced with permission.

The number of OH^- ions and the acidity of superficial groups, strongly influence the electronic environment of the Ti cations. [11,23] The hydrated surface is described as a series of Ti^{4+} and O^{2-} ions, where the Ti cations can exist at different crystallographic planes. The dissociative chemisorption of water at TiO_2 surface leads to the formation of three potential binding sites around Ti atom, denote as A, B, C. As pictured in Fig. 3, the green A sites display a hexacoordinated titanium atom with five bridging oxo (O^{2-}) anions and a hydroxyl (OH^-) ligand;

the blue *B* sites show a OH⁻ forming a bridge between two Ti ions, and the red *C* binding sites are present at the edges and corners of the crystal with four oxo ligands. [11]

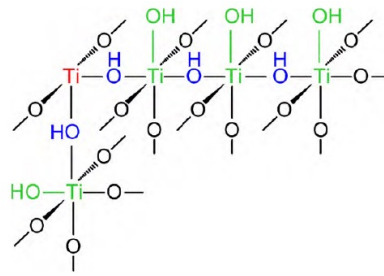


FIGURE 3. Binding sites of Ti at the surface of TiO₂, where *A* green; *B* blue; *C* red. From [11], reproduced with permission.

The chemisorption of organic compounds on TiO₂ surface can be considered as Lewis and/or Brønsted acid/base reaction. Donor groups such as oxygen, nitrogen or sulfur atoms could act as a Lewis base, and donate electrons to Ti⁴⁺ ions in the surface (Lewis acid). [11] Hence, three principal coordination modes exist, as noted in Fig. 4, monodentate, bidentate chelating and bidentate bridging. Additionally, the structure and stability of the complex formation onto TiO₂ surface are also fine-tuned by the crystallographic plane, accessibility to Ti ions, type of organic ligands, and pH.

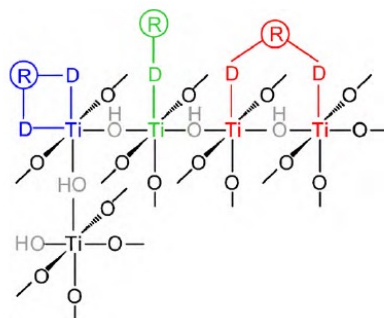


FIGURE 4. Coordination modes in the TiO₂ surface: monodentate (green), bidentate chelating (red), bidentate bridging (blue). From [11], reproduced with permission.

Thermodynamic considerations

Rutile is the most stable phase at high temperatures, whereas anatase and brookite are largely common to nanometric scale in natural or synthetic form. Whether an excessive heating is made, several phase transformations occur: from anatase to brookite to rutile, from brookite to anatase to rutile, from anatase to rutile and from brookite to rutile. These transformations imply an energetic balance as a function of the particle size. So the enthalpy of the three polymorphic phases is different enough to bring about changes in terms of thermodynamic stability. [19]

Hwu and coworkers reported that the crystalline structure of TiO₂ nanoparticles depends strongly on the preparation method. [24] For instance, small particles of anatase phase (< 50 nm) are seemingly more stable and transform to rutile at higher temperatures (> 700 °C), however, Banfield and Zhang prepared TiO₂ nanoparticles with an anatase and/or brookite phase, and

demonstrated that upon reaching a certain particle size it can transform to rutile. Interestingly, once it forms, it grows faster than anatase. Thus, rutile becomes more stable than anatase in particle sizes up to 14 nm. [24-25]

Likewise, Zhang *et al.* measured by differential thermogravimetric calorimetry and x-ray diffraction (XRD) analysis, a slow phase transition from brookite (prepared by a wet chemical method) to anatase under 780 °C, in which the grains slowly grow between 780-850 °C, coexisting a rapid transformation of brookite to anatase then to rutile. Hence, brookite cannot be transformed directly to rutile, because it firstly needs forming the anatase phase. [26] On the other hand, Kominami *et al.*, synthesized a brookite-type TiO₂ by thermal treatment of Ti(acac)₂ (acac = acetylacetonate) in ethylene glycol (EG) in the presence of sodium laurate and a small amount of water, demonstrating the direct transformation of brookite-nanocrystals to rutile above 700 °C. [27]

Electronic considerations

The molecular orbital diagram for anatase TiO₂ (Fig. 5) comprises of titanium (4s and 3d) and oxygen (2s and 2p) atomic orbitals. In the former case, they split into higher energy crystal-field e_g and t_{2g} configuration, and triply degenerate d_{xz} , d_{yz} and d_{xy} levels; while the oxygen atom has the orbitals p_π and p_σ . The resulting states of interaction have the nonbonding orbital p_π at the top of the valence band and the nonbonding orbital d_{xy} at the bottom of the conduction band. [28] Such a feature is also observed in the rutile phase, but is less noteworthy than anatase. [29]

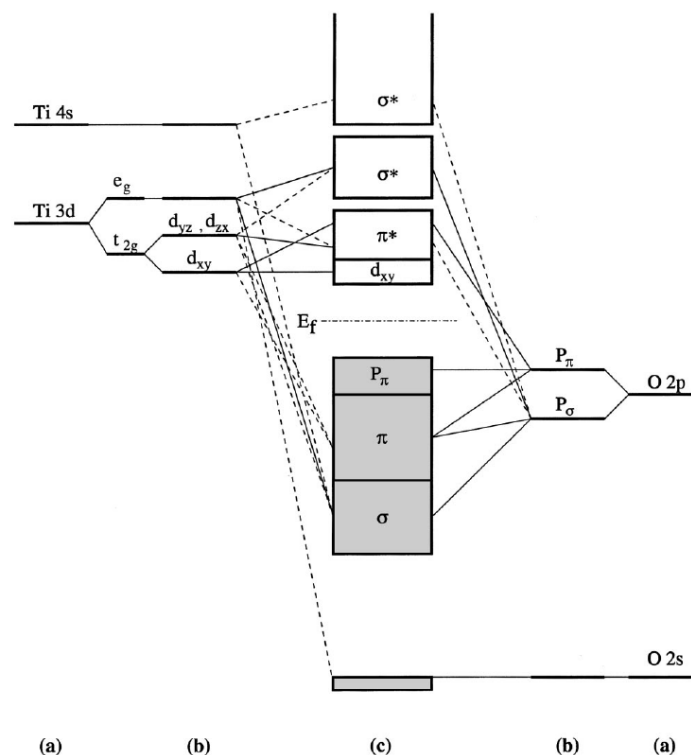


FIGURE 5. Molecular orbital energy diagram for TiO₂ anatase phase, where (a) atomic orbitals; (b) crystal-field interactions; and (c) final interaction states. From [28], reproduced with permission.

It follows that anatase phase is less dense than rutile, because the later forms linear chains, where each octahedra share eight neighbor atoms in the corners and two neighbor atoms at edges. Conversely, the anatase polymorph leads to zigzag chains with a screw axis, whose octahedra both share four corners and edges of four neighbors. [19]

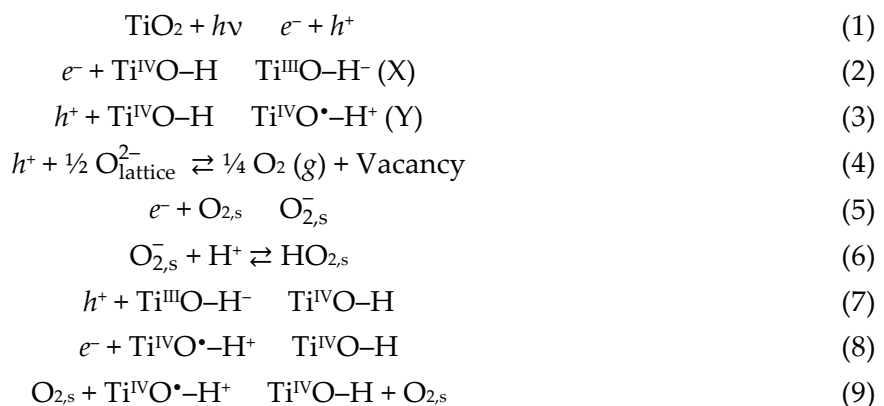
The d_{xy} orbital of anatase on the bottom of the conduction band is more isolated because this phase has a large metal-metal distance (5.35 Å); while rutile has a smaller metal-metal distance of 2.96 Å due to t_{2g} orbital is on the bottom of the conduction band. [19].

Optical features

In semiconductors such as germanium and silicon atoms, the main light absorption mechanism occurs by directly inter-band electron transitions; but in the case of indirect semiconductor, as TiO₂, the absorption is smaller due to crystal symmetry constraints affecting direct transitions of electrons between bands. [19] Braginsky and Shklover showed that the possibility of momentum non-conservation at the interface causes the indirect inter-band electron transition, a trait important in crystals of less than 10 nm. [30] With unequal interfaces there is better contact of atoms that greatly enhance the effect previously noted. The indirect transitions are allowed because the large density of states for the electrons in the valence band. [19]

As the interface contact of atoms is large enough, a considerable improve in the absorption is expected in microcrystalline and porous TiO₂. At low photon energies, a rapid increase in the absorption is observed, due to an enhancement of the electron density of states only seen in the valence band; and in crystallites smaller than ~20 nm, the interface absorption becomes the most important mechanism of light absorption. [30]

When TiO₂ nanoparticles absorb photons with energy equal or greater than the prohibited band (> 3 eV), the electrons in the valence band are excited to the conduction band, leaving behind a positive hole in the valence band. These electrons can recombine or stay trap and react with donor/acceptor electrons absorbed in the surface of the photocatalyst. The competition among these processes has to do with the efficiency of numerous applications of TiO₂ nanoparticles. Such photogenerated electrons e^- and holes h^+ (exciton) disperse to the surface and can be expressed as follows: [31]



The first reaction (1) is a process of photon absorption, reactions (2)-(6) represent photocatalytic redox pathways, (7)-(9) are recombination channels, reaction (3) and (4) compete for holes, leading to bound OH radicals and O vacancies. The reverse of (4), generates O atoms that are on the crystal surface (adatom intermediate) upon exposing defective surfaces to O^{2-} (g). [31]

The electrons and holes in TiO_2 nanoparticles have different defect sites on the surface and in the bulk. [19] Howe and Grätzel investigated species formed on irradiation of TiO_2 at -269 °C in vacuum, it was shown by electron paramagnetic resonance (EPR) that the electrons are trapped between Ti^{4+} species produced by band-gap irradiation in the presence of suitable hole scavengers, but in the absence of hole scavengers, the species are trapped only at the interior sites with interstitial Ti^{4+} species unstable at room temperature. [32-33] Interestingly, Thurnauer and coworkers used EPR to investigate electron transfer within a mix-phase TiO_2 sample where charge migration and recombination at the surface sites on TiO_2 occur upon band gap illumination, giving rise to hole formation at the surface and preferentially recombination with electrons in surface trapping sites. [34]

III. SURFACE MODIFICATION OF TiO_2

To improve the physicochemical features (e.g., efficiency and functionality) of TiO_2 -based nanomaterials one modifies the optical properties, since the bandgap of titanium dioxide is in the ultraviolet region of the solar spectrum and represents only a fraction of 10%. Rutile has a direct bandgap of 3.06 eV and an indirect bandgap of about 3.10 eV, while anatase exhibits only an indirect bandgap at 3.23 eV. [35,36] (Fig. 6). Therefore, much of the research focuses on changing the response from the UV to the visible region.

In this regard, Chen and Mao suggested some pathways that allow improving the optical activity of TiO_2 nanomaterials by shifting the UV light to visible: Upon doping with compounds affects the optical features, by sensibilization with inorganic or organic compounds; and coupling of collective oscillations of the electrons in the conduction of metal nanoparticles surface alongside those in the conduction band of TiO_2 . [19]

Chemical modifications

Doping. By doping a semiconductor one introduces impurities into the device to modify its electrical response. In the case of TiO_2 , one induces a decrease of the band gap having a response in the absorption of further visible light. [37] Indeed, such approach leads an improvement in the catalytic activity. Besides, the replacement of oxygen and titanium atoms prompts changes in the optical response, but maintaining the integrity of the crystal structure of the photocatalyst and varying its electronic structure. [19,37]

The substitution of Ti^{4+} ions in TiO_2 is feasible with other transition metal cations than to substitute O^{2-} with other anions because of the difference in the charge states and ionic radii. [38] The small size of the nanoparticles shows a higher tolerance to structural distortion for the modification of the TiO_2 composition, than that of bulk materials due to their inherent lattice

strain. [39,40] The synthesis, properties and types of TiO₂-doped are reviewed elsewhere. [19,37,41-43]

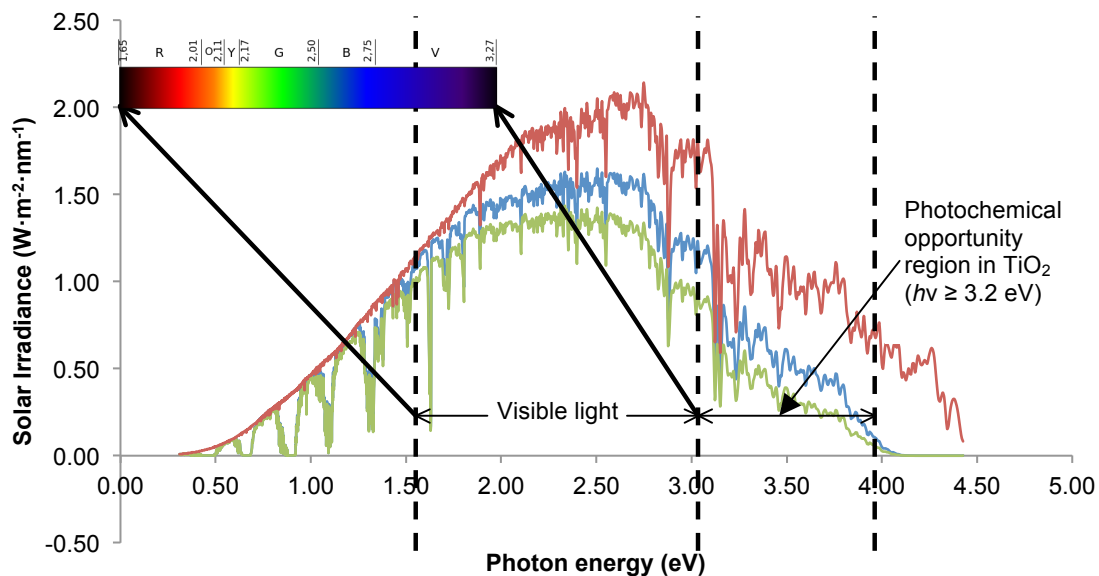


FIGURE 6. Solar spectral irradiance, where — Global tilt (spectral radiation from solar disk plus sky diffuse and diffuse reflected from ground on south facing surface tilted 37° from horizontal). — Direct (direct normal irradiance nearly parallel) + Circumsolar (spectral irradiance within ±2.5° field of view centered on the 0.5° diameter solar disk, but excluding the radiation from disk). — Extraterrestrial radiation (solar spectrum at top of atmosphere at mean Earth-Sun distance). (Numerical data from ASTM G173-03 Reference Spectra)

Chemical modification at the TiO₂ surface. As described previously, TiO₂ is a semiconductor with a wide band gap which absorbs light in the UV region; when it is modify with a dye a photocurrent is generated with light energy less than that of the semiconductor band gap, the process is known as sensitization and the light-absorbing dyes are named sensitizers. [19] These materials can be inorganic semiconductors with narrow band gaps, metal nanoparticles, organometallic and organic compounds.

The light-conversion efficiency depends greatly on the interaction of the sensitizers with the incoming light. Light excitation by coordination compounds, anchored to TiO₂, can initiate an electron-transfer process from the sensitizer to titanium dioxide, which ultimately reduces the semiconductor; resulting in a charge separation process; which is relevant for solar energy conversion. [44]

Organometallic dyes for sensitization. Since the pioneering work from Grätzel and O'Regan in dye-sensitized solar cells (DSSCs, also known as third-generation solar cells) [45], a great variety organic dyes have been employed as sensitizer for TiO₂ nanomaterials.

Depending on the type of organic/organometallic compound, the way of anchoring of the titanium dioxide varies, since the presence of certain functional groups influence the interaction

between the dye and the substrate. The nature of such interactions is as follows: covalently bonds, electrostatics, hydrogen bonding, van der Waals forces, inclusion or entrapment in cavities or pores, etc. [46]

Sensitizer molecules have anchoring groups such as silanyl, ($-\text{O}-\text{Si}-$), amide ($-\text{NH}-(\text{C}=\text{O})-$), carboxyl ($-\text{O}-(\text{C}=\text{O})-$), phosphonato ($-\text{O}-(\text{HPO}_2)-$), featuring stable linkages at TiO_2 surface. (Fig. 7) [46]

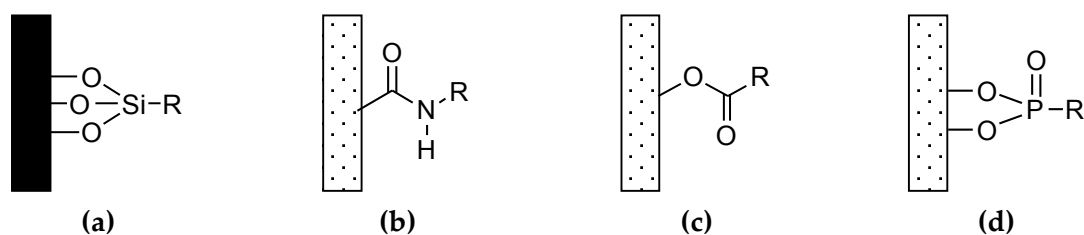


FIGURE 7. Scheme of the different linker groups.
(a) Silanyl; (b) amide; (c) carboxyl; (d) phosphonato.

Cyano-metal complexes in acid solutions also act as linker moiety, for instance, Meyer and co-workers tailored $\text{Na}_2[\text{Fe}(\text{bpy})(\text{CN})_4]$, (where bpy = 2,2'-bipyridine) to TiO_2 , through a single cyanide ligand with a C_{4v} symmetry, as $\text{Ti}^{\text{IV}}-\text{NC}-\text{Fe}^{\text{II}}(\text{CN})_3$. [47] (Fig. 8)

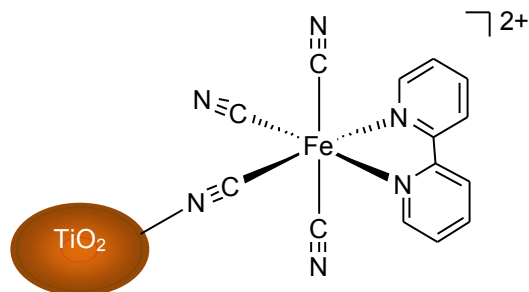


FIGURE 8. Schematic representation of the linkage $\text{Ti}^{\text{IV}}-\text{NC}-\text{Fe}^{\text{II}}(\text{CN})_3$.

The mechanism of interfacial charge separation differs by the type of donor that transfers the electron to the TiO_2 : [44]

- Excited state
- Reduced state
- Molecule-to-particle charge-transfer complex.

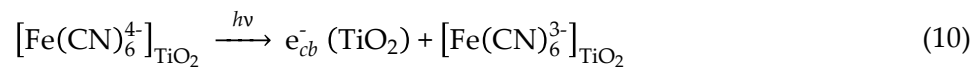
The electron transfer mechanism in dye-sensitized TiO_2 mostly takes place by metal-to-ligand charge transfer (MLCT) from the central metal atom to unoccupied molecular orbitals of the ligands, especially in metals with highly filled d orbitals, which enable the transfer of electrons to

antibonding orbitals at ligands. [48-50] Moreover, the nonbonding *d* orbitals should be similar to the antibonding orbitals in terms of size, shape and symmetry. [51]

An efficient photosensitizer should meet several requirements: [19,52,53]

- a. An absorption spectrum covering the whole visible, infrared and near-infrared region.
- b. Anchoring groups for strongly linkages between the photosensitizer and the semiconductor.
- c. The excited states of the dye should have a long lifetime and high quantum yield.
- d. An energy-level orbital position similar between the dyes and the semiconductor to ensure an efficiency charge transfer. [54]

The electron transfer from the dye to TiO₂ nanoparticles is usually very fast, from tens to femtoseconds. The mechanism of MLCT involves an interfacial phenomenon, as noted by Grätzel and coworkers, that described a very rapid photoinduced electron injection into the conduction band (*cb*) of TiO₂ [reaction (10)], following a much slower intra-particle back electron transfer [reaction (11)] to the metal-organic dye. [55]



Searson *et al.* studied the photocurrent response of dye-sensitized porous nanocrystalline TiO₂ cells and found that the electron transport can be explained by a diffusion model. [56] In the same line, de Jongh and Vanmaekelbergh demonstrated that electron transport is controlled by trapping and detrapping of photogenerated electrons in the interfacial bandgap, and the localization time of a trapped electron was controlled by the steady-state light intensity and interfacial kinetics, in assemblies of nanometric-size TiO₂, measured by intensity-modulated photocurrent spectroscopy (IMPS). [57]

IV. BRIDGE-LIKE MOLECULES TO IMMOBILIZE SENSITIZER MOLECULES IN NANOPARTICULATE TiO₂

As depicted in the electronic cycle of a DSSC (Fig. 9), the photoanode is made of a transparent conductive oxide of SnO₂:F (FTO), a film of nanoparticle TiO₂ and covalently bonding of a dye, that upon light irradiation causes a photoexcitation process, followed by quickly injection of electrons in the conduction band of the semiconductor; this first step (from a series of electrons transfer process) results in the production of electric energy using 1.5 Air-Mass conditions (1000 W/m²) or Sun light. Additionally, there is an electrolyte redox mediator solution (I⁻/I₃⁻) and a transparent photocathode coated by thin film of graphite or Pt. DSSCs have attracted much attention as a way to decrease cost production. [45,52,53,58-63]

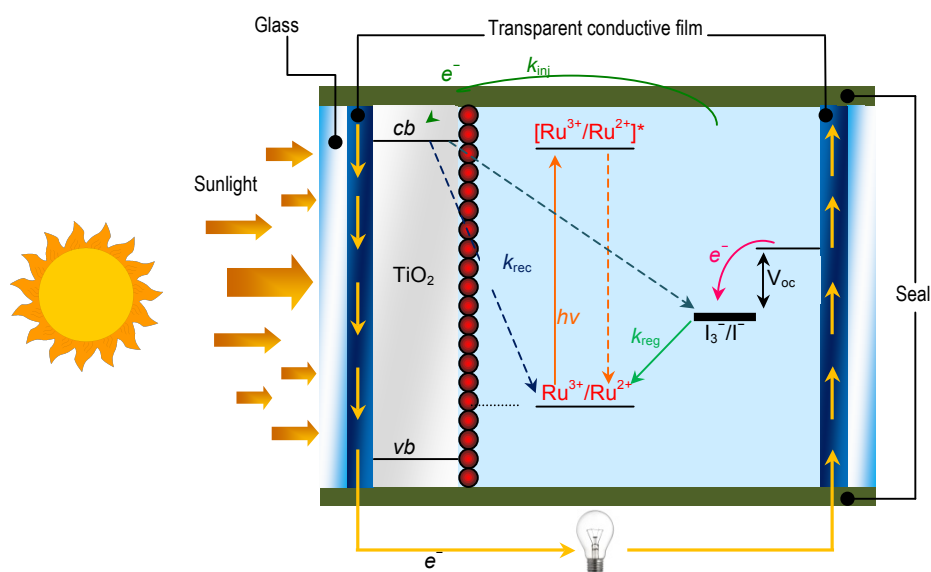


FIGURE 9. Scheme of the electronic process in DSSC, using a $\text{Ru}^{3+}/\text{Ru}^{2+}$ dye, anchored to TiO_2 ; where $h\nu$ photoexcitation of the dye and formation of the lowest excited state, a MLCT transition; k_{inj} electron injection; k_{rec} recombination; k_{reg} reduction of Ru^{3+} by a redox mediator (dye regeneration with I_3^-/I^- electrolyte); cb conduction band; vb valence band; V_{oc} open circuit voltage. Dotted arrows show competing processes.

DSSCs have the advantage of tunable optical features, and facile to assembly. More recently, Grätzel *et al.* reported on a dye-sensitized solar device highly efficient (13%) using an organometallic dye depicted in Fig. 10, and cobalt(II/III) as redox shuttle, showing promising physicochemical parameters of open-circuit voltage $V_{\text{oc}} = 0.91$ V, short-circuit current density $J_{\text{sc}} = 18.1$ mA/cm^2 , and fill factor of 0.78. [64]

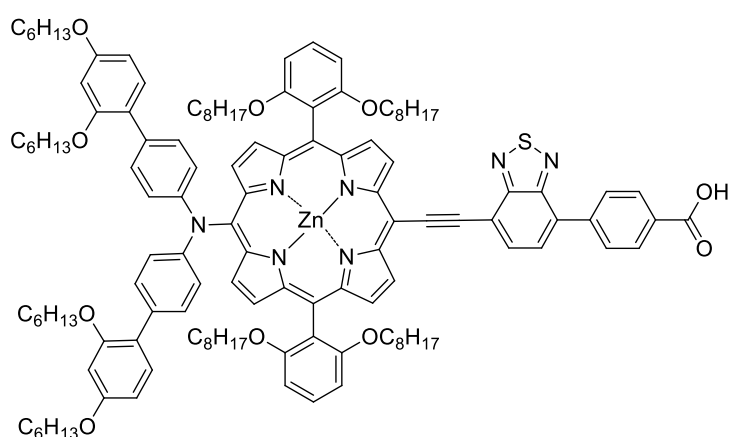


FIGURE 10. Dye molecular composition for DSSC with 13% efficiency. The structure features a porphyrin core and a bulky bis(2',4'-bis(hexyloxy)-[1,1'-biphenyl]-4-yl)amine donor and a benzothiadiazole acceptor group.

In general, designing linker molecules facilitate the anchoring of the dye with the semiconductor in sensitizer-bridge-anchor arrays, as shown in Fig. 11. Metal-polypyridine complexes are important sensitizer for thin film electrodes because of the strongly absorption in the visible region, long excited state lifetimes, oxidized and reduced stable forms, and the tendency to avoid the formation of aggregates or degradation with time. [62] Also, it has been successfully tested molecules such as porphyrins, phthalocyanines, viologens, and bipyridines in DSSCs, in table I, are summarized some examples of dyes for DSSCs and their conversion efficiencies.

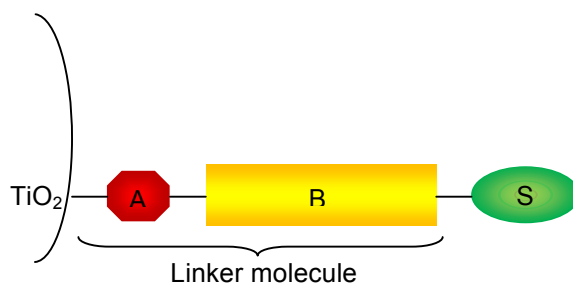


FIGURE 11. Schematic representation of a bridge-like molecule, used to bind sensitizer to the semiconductor surface; where A is the anchoring group(s), B bridge, S sensitizer molecule.

In early experiments, the dyes were absorbed by physisorption means leading to low efficiencies, so it became important to control the bonding process. To this end, the preparation of dye molecules bearing anchoring groups harnesses covalent bonding interactions by strengthening of the electronic coupling between the molecular orbital of the dye and the band gap of the semiconductor, leading to fast injection rates of electrons. As such, there is an improvement regarding surface coverage of the sensitizer, stability, less desorption pathways, and a better distribution of the dye that forms a monolayer in the TiO_2 . [62]

In titanium dioxide, a saturated bridge between the chromophore and the bonding group weakens the electronic coupling and reduce the electron injection rate, which highlights the use of covalent bonds for anchoring dyes.

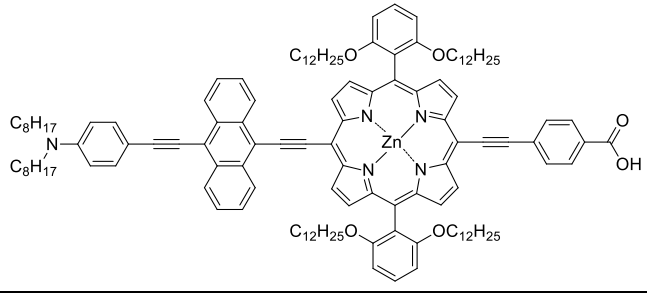
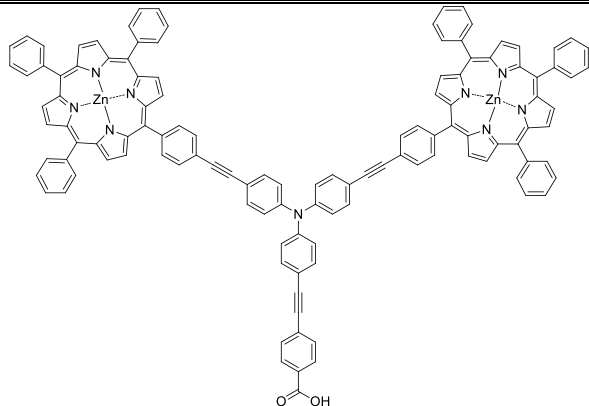
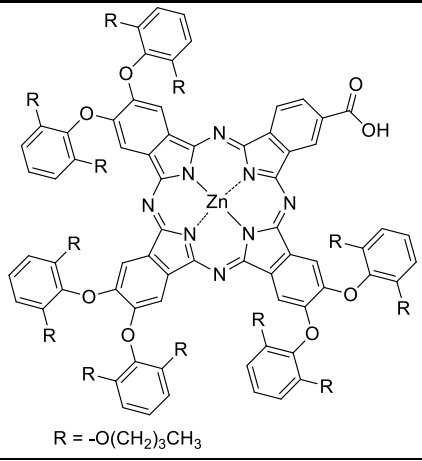
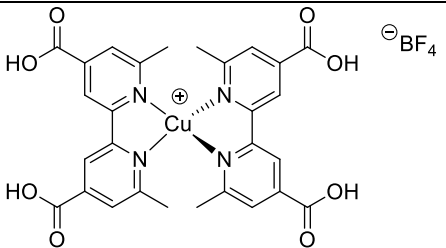
To design and study bridge molecules in dye-semiconductor interface, currently investigations are based on: [62]

- a. Organic-bridged molecules that serve for mechanistic studies.
- b. Systematic variation on the distance and orientation of the sensitizer at the surface, with bridge of different lengths, to study the dependence of the distance.
- c. Linker molecules with large surface area that prevent dye aggregation.
- d. Linker molecules with different functional groups that vary the chromophore properties like the absorption spectra in visible region and to rise the molar extinction coefficient.
- e. Bridge molecules that can change the chemical surface.

Anchoring group features

In general, for metallic oxides, anchoring groups like phosphoric and carboxylic acids, as well as their derivatives (e.g., esters, acid chlorides, carboxylate salts or amides) thermodynamically bind to the surface. However, under basic conditions (usually $\text{pH} \geq 9$) the dye molecules easily detach from the oxide surface. [46,62,69]

TABLE I. Molecule dyes in DSSCs.

Type of dye	Structure	Efficiency % η	Reference
		10.3%	[65]
Porphyrin		0.31%	[66]
Phthalocyanine	 <p>R = -O(CH₂)₃CH₃</p>	6.4%	[67]
Bipyridine		0.83%	[68]

In this sense, the immobilization of stearic acid onto TiO₂ anatase (101) surface by using microwave heating, changes the wettability of the oxide, as observed in Fig. 12, the reaction (12) renders a hydrophobic surface (114°), as demonstrated by contact angle measured in water. [70]

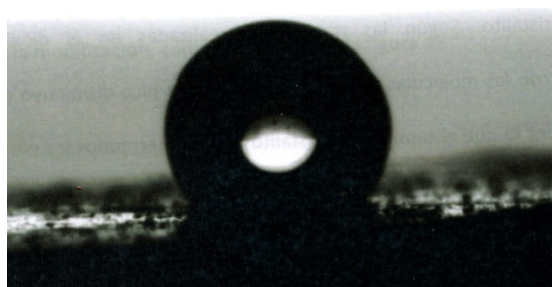
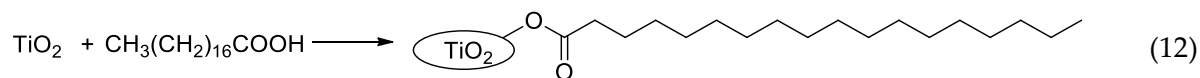
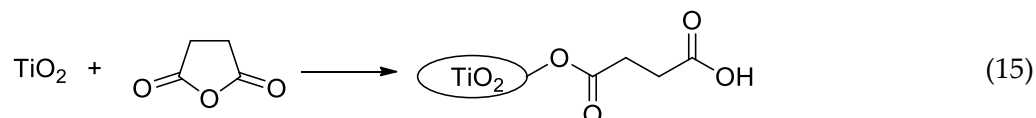
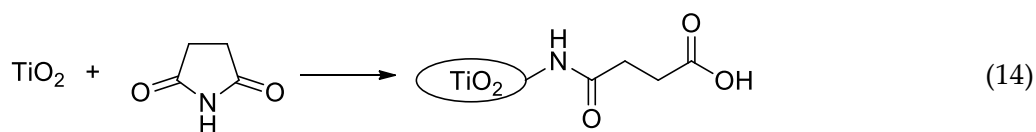
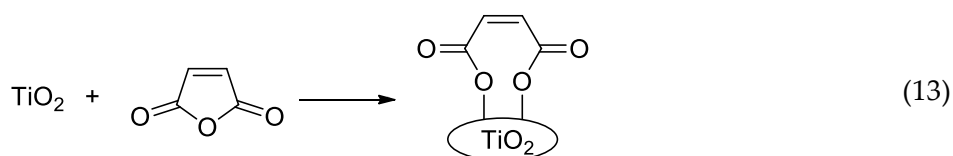


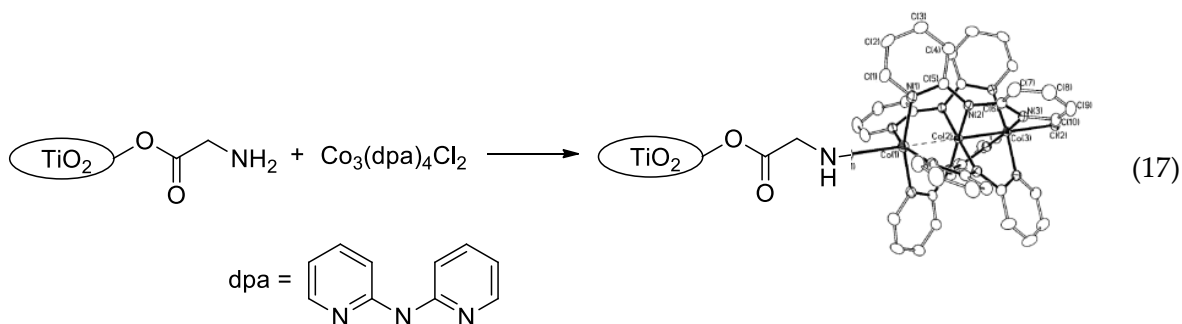
FIGURE 12. Contact angle water-drop shape of the TiO₂-stearic acid modification. From [69], reproduced with permission.

In the case of cyclic molecules, like maleic anhydride (13), succinimide (14) and succinic anhydride (15) in the presence of TiO₂, behave as dicarboxylic acids and double-end terminal amine-carboxylic acid fragment upon open-ring reaction [(13)-(15)]. Structurally, there is a restriction in maleic anhydride imposed by *cis* double bond preventing the bonding through a single -COOH group; instead a cyclization product is obtained. But, in the case of succinimide and succinic anhydride molecules no cyclization at surface is attained. [70]



Using molecules with two or more anchoring groups have the advantage to further bonding other molecules that enhance the absorption characteristic of the titanium dioxide, as shown in Fig. 11. Intriguingly, upon first glycine molecule attachment as linker fragment to TiO₂, it leaves a free amine group (16), which can coordinate further to transition metal complexes. Such

synthetic approach has been used to tether multinuclear cobalt complexes (17) onto TiO_2 , a functional substrate that shows photocatalytic activity for the water reduction reaction. [70,71]



V. APPLICATIONS OF TiO_2 FOR THE DEVELOPMENT OF PHOTOELECTROCHEMICAL CELLS IN WATER OXIDATION REACTION

The first example of a water-splitting reaction by a photoelectrochemical method was reported by Fujishima and Honda in 1972; it was used TiO_2 as a photoanode under illumination of UV light, with gas evolution of oxygen in the anode and hydrogen in a platinum cathode without illumination. [9] Because of this work, a great deal of effort is being carried out to modify the TiO_2 surface to have higher catalytic activity.

At present, one of the most interesting areas is developing photoelectrochemical devices that operate under working principles of DSSCs to perform the water oxidation reaction to produce O_2 and H_2 . As depicted in Fig. 13, it has several features: an efficient light-harnessing system, components for charge separation, a robust water-oxidation catalyst that is able to transfer four electrons and facilitates the formation of O–O bonding. [72,73]

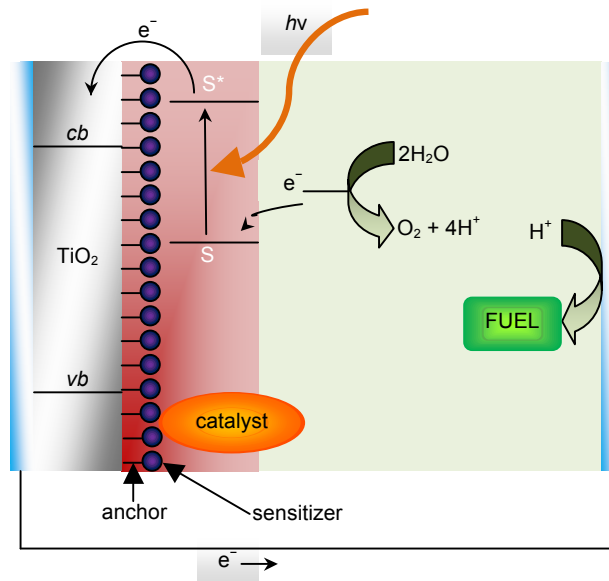


FIGURE 13. Photoelectrolytic device for the production of solar fuels from water oxidation reaction.

Mallouk and coworkers, reported on mesoporous TiO₂ as photoanode (like DSSC) using a [Ru(bpy)₃]²⁺ dye, and anchoring IrO₂·nH₂O particles as water oxidation catalyst [74], as pictured in Fig. 14. The system consists of TiO₂-dye-IrO₂ photoanode and platinum (Pt) wire as cathode where H⁺ reduces to H₂. Nevertheless, this configuration has low quantum efficiency (1%), and a turnover-number (TON) of about 16.

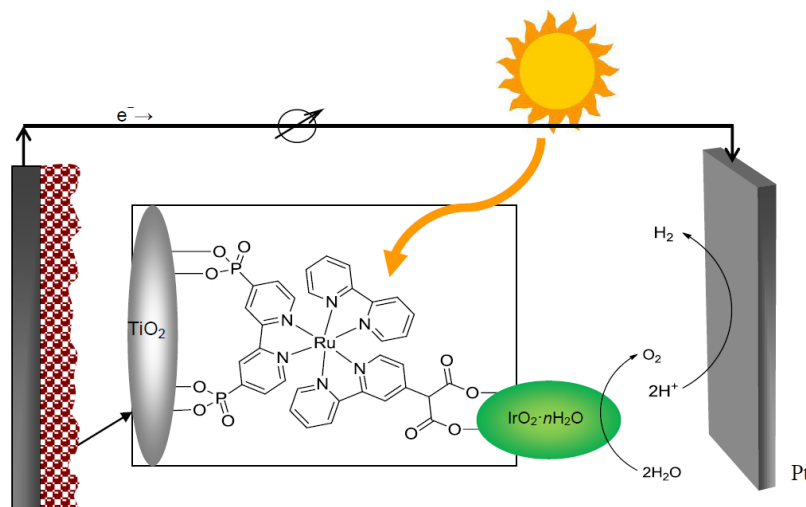


FIGURE 14. Photoelectrochemical device for the water-splitting reaction with IrO₂·nH₂O nanoparticles as a catalyst, using DSSC principle with a ruthenium-dye anchored onto TiO₂.

Spiccia *et al.* synthesized an oxo-manganese cluster [Mn₄O₄L₆]⁺, (L = (MeOPh)₂PO₂⁻), that was combined in a Nafion[®] membrane as a catalyst, along with a ruthenium dye [Ru^{II}(bpy)₂(bpy(COO)₂)] tailored in TiO₂ in a fluorine-doped thin oxide electrode. [75] (Fig. 15)

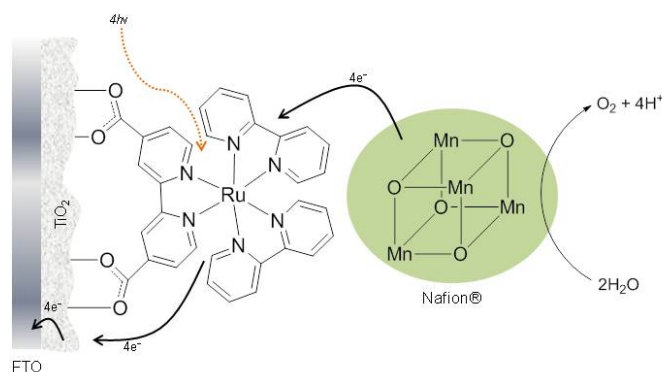


FIGURE 15. Photoelectrochemical cell with an oxo-Mn cubane in Nafion[®], using a Ru-dye photosensitizer in a TiO₂ surface.

When light energy is absorbed by Ru^{II} complex, it injects electrons in the conduction band of TiO₂, flowing through an external circuit leaving a Ru^{III} dye capable of reduce the cubane structure. Such reduced form of the Mn-cluster has the electrochemical potential necessary to oxidize the water molecule and generates O₂, while the protons are reduced in a Pt electrode that releases H₂. [74]

VI. CONCLUDING REMARKS

The stability and surface robustness in TiO₂ against photo-corrosion and degradation have been widely studied and applied in several important applications. Such features are of great advantage over other binary oxides that easily decomposed under similar conditions (e.g., SnO₂, ZnO). Additionally, its surface atomic composition has a rich electronic situation for further surface functionalization. Novel optical features have been attained by modifying TiO₂ nanomaterial surface to synthesize photocatalysts aiming at solar fuels production, so that solar energy can be harnessed. Hence, optical sensibility and activity can be raised by band-gap engineering, doping or anchoring of organic-inorganic sensitizers to absorb in the visible light and near-infrared region. The functionalization of TiO₂ nanoparticles has proved to be a successful approach to devise new materials with new characteristics that could in the short-run alone with other technologies cope with environmental and energy challenges facing humanity.

Indeed, with actual global energy consumption and dwindling of fossil fuel reserves, it is expected that TiO₂-based nanomaterials take advantage of Sun light, especially in the implementation of photoelectrochemical devices in a global scale. However, much of the development in DSSCs as well as photoelectrochemical devices relies on expensive and scanty ruthenium dyes, or chromophore molecules with complex synthetic steps, and systems with low energy efficiencies; this turns out decision making doubt about their large-scale implementation, such that further research is still needed to foster sustainable solar fuel initiatives.

VII. REFERENCES

- [1] Sibum, H.; Güther, V.; Roidl, O.; Habashi, F.; Wolf, H. U. Titanium, titanium alloys, and titanium compounds, in *Ullmann's Encyclopedia of Industrial Chemistry*, Wiley-VCH: Weinheim, 2000.
- [2] Buxbaum, G.; Pfaff, G. *Industrial Inorganic Pigments*, 3rd ed. Wiley-VCH: Weinheim, 2005, pp. 51-76.
- [3] Pfaff, G.; Reynders, P. *Chem. Rev.* **1999**, *99*, 1963-1982.
- [4] Schilling, K.; Bradford, B.; Castelli, D.; Dufour, E.; Nash, J. F.; Pape, W.; Schulte, S.; Tooley, I.; van den Bosch, J.; Schellauf. *Photochem. Photobiol. Sci.* **2010**, *9*, 495-509.
- [5] Singh, S.; Nalwa, H. S. *J. Nanosci. Nanotechnol.* **2007**, *7*, 3048-3070.
- [6] Yuan, S. A.; Chen, W. H.; Hu, S. S. *Mater. Sci. Eng. C* **2005**, *25*, 479-485.
- [7] Weir, A.; Westerhoff, P.; Fabricius, L.; Hristovski, K.; von Goetz, N. *Environ. Sci. Technol.* **2012**, *46*, 2242-2250.
- [8] Tian, Y. F.; Hu, S. J.; Yan, S. S.; Mei, L. M. *Chin. Phys. B* **2013**, *22*, 088505.
- [9] Fujishima, A.; Honda, K. *Nature* **1972**, *238*, 37-38.
- [10] Concepción, J. J.; House, R. L.; Papanikolas, J. M.; Meyer, T. J. *Proc. Natl. Acad. Sci. U.S.A.* **2012**, *109*, 15560-15564.
- [11] Macyk, W.; Szaciłowski, K.; Stochel, G.; Buchalska, M.; Kuncewicz, J.; Łabuz, P. *Coord. Chem. Rev.* **2010**, *254*, 2687-2701.
- [12] Habisreutinger, S. N.; Schmidt-Mende, L.; Stolarczyk, J. K. *Angew. Chem. Int. Ed.* **2013**, *52*, 7372-7408.
- [13] Kisch, H. *Angew. Chem. Int. Ed.* **2013**, *52*, 812-847.
- [14] Roy, P.; Berger, S.; Schmuki, P. *Angew. Chem. Int. Ed.* **2011**, *50*, 2904-2939.
- [15] Park, H.; Park, Y.; Kim, W.; Choi, W. *J. Photochem. Photobiol. C: Photochem. Rev.* **2013**, *15*, 1-20.
- [16] Xu, Q.; Zhang, J.; Feng, Z.; Ma, Y.; Wang, X.; Li, C. *Chem. Asian J.* **2010**, *5*, 2158-2161.
- [17] Diebold, U. *Surf. Sci. Rep.* **2003**, *48*, 53-229.
- [18] Uberuaga, B. P.; Bai, X. M. *J. Phys.: Condens. Matter* **2011**, *23*, 435004.
- [19] Chen, X.; Mao, S. *Chem. Rev.* **2007**, *107*, 2891-2959.
- [20] Pierre, A.; Pajonk, G. *Chem. Rev.* **2002**, *102*, 4243-4266.
- [21] Swamy, V.; Kuznetsov, A.; Dubrovinsky, L.; Caruso, R.; Shchukin, D.; Muddle, B. *Phys. Rev. B.* **2005**, *71*, 184302/1.
- [22] Srivastava, A. K.; Deepa, M.; Bhandari, S.; Fues, H. *Nanoscale Res. Lett.* **2009**, *4*, 54-62.
- [23] Tunesi, S.; Anderson, M. *J. Phys. Chem.* **1991**, *95*, 3399-3405.
- [24] Hwu, Y.; Yao, Y. D.; Cheng, N. F.; Tung, C. Y.; Lin, H. M. *Nanostruct. Mater.* **1997**, *9*, 355-358.
- [25] Zhang, H.; Banfield, J. F. *J. Mater. Chem.* **1998**, *8*, 2073-2076.
- [26] Ye, X.; Sha, J.; Jiao, Z.; Zhang, L. *Nanostruct. Mater.* **1997**, *8*, 919-927.
- [27] Kominami, H.; Kohno, M.; Kera, Y. *J. Mater. Chem.* **2000**, *10*, 1151-1156.
- [28] Asahi, R.; Taga, Y.; Mannstadt, W.; Freeman, A. J. *Phys. Rev. B* **2000**, *61*, 7459-7465.

- [29] Sorantin, P. I.; Schwarz, K. *Inorg. Chem.* **1992**, *31*, 567-576.
- [30] Braginsky, L.; Shklover, V. *Eur. Phys. J. D* **1999**, *9*, 627-630.
- [31] Szczepankiewicz, S. H.; Colussi, A. J.; Hoffmann, M. R. *J. Phys. Chem. B* **2000**, *104*, 9842-9850.
- [32] Howe, R. F.; Grätzel, M. *J. Phys. Chem.* **1985**, *89*, 4495-4499.
- [33] Howe, R. F.; Grätzel, M. *J. Phys. Chem.* **1987**, *91*, 3906-3909.
- [34] Hurum, D. C.; Agrios, A. G.; Crist, S. E.; Gray, K. A.; Rajh, T.; Thurnauer, M. C. *J. Electron Spectrosc. Relat. Phenom.* **2006**, *150*, 155-163.
- [35] Valencia, S.; Marín, J. M.; Restrepo, G. *Open Mater. Sci. J.* **2010**, *4*, 9-14.
- [36] Welte, A.; Waldauf, C.; Brabec, C.; Wellmann, P. J. *Thin Solid Films* **2008**, *516*, 7256-7259.
- [37] Mital, G. S.; Manoj, T. *Chinese Sci. Bull.* **2011**, *56*, 1639-1657.
- [38] Mor, G. K.; Varghese, O. K.; Paulose, M.; Shankar, K.; Grimes, C. A. *Solar Energ. Mater. Solar Cell* **2006**, *90*, 2011-2075.
- [39] Burda, C.; Lou, Y.; Chen, X.; Samia, A. C. S.; Stout, J.; Gole, J. *Nano Lett.* **2003**, *3*, 1049-1051.
- [40] Chen, X.; Lou, Y.; Samia, A. C. Burda, C. *Nano Lett.* **2003**, *3*, 799-803.
- [41] Wang, H.; Lewis, J. P. *J. Phys.: Condens. Matter* **2006**, *18*, 421-434.
- [42] Umabayashi, T.; Yamaki, T.; Itoh, H.; Asai, K. *Appl. Phys. Lett.* **2002**, *81*, 454-456.
- [43] Dunnill, C. W.; Parkin, I. P. *Dalton Trans.* **2011**, *40*, 1635-1640.
- [44] Meyer, G. J. *Inorg. Chem.* **2005**, *44*, 6852-6864.
- [45] O'Regan, B.; Grätzel, M. *Nature* **1991**, *353*, 737-740.
- [46] Kalyanasundaram, K.; Grätzel, M. *Coord. Chem. Rev.* **1998**, *77*, 347-414.
- [47] Yang, M.; Thompson, D. W.; Meyer, G. J. *Inorg. Chem.* **2000**, *39*, 3738-3739.
- [48] Argazzi, R.; Bignozzi, C.; Heimer, T.; Castellano, F.; Meyer, G. J. *Phys. Chem. B* **1997**, *101*, 2591-2597.
- [49] Hannappel, T.; Burfeindt, B.; Storck, W.; Willing, F. *J. Phys. Chem. B* **1997**, *101*, 6799-6802.
- [50] Heimer, T.; Heilweil, E. J. *Phys. Chem. B* **1997**, *101*, 10990-10993.
- [51] Arifin, K.; Majlan, E. H.; Wan Daud, W. R.; Kassim, M. B. *Int. J. Hydrogen Energy* **2012**, *37*, 3066-3087.
- [52] Hagfeldt, A.; Boschloo, G.; Sun, L.; Kloo, L.; Pettersson, H. *Chem. Rev.* **2010**, *110*, 6595-6663.
- [53] Barea, E. M.; Bisquert, J. *Langmuir* **2013**, *29*, 8773-8781.
- [54] Hao, Y.; Yang, X.; Cong, J.; Jiang, X.; Hagfeldt, A. Sun, L. *RSC Adv.* **2012**, *2*, 6011-6017.
- [55] Vrachnou, E.; Vlachopoulos, N.; Grätzel, M. *J. Chem. Soc., Chem. Commun.* **1987**, 868-870.
- [56] Cao, F.; Oskam, G.; Meyer, G. J.; Searson, P. C. *J. Phys. Chem.* **1996**, *100*, 17021-17027.
- [57] de Jongh, P. E.; Vanmaekelbergh, D. *Phys. Rev. Lett.* **1996**, *77*, 3427-3430.
- [58] Grätzel, M. *Chem. Ing. Tech.* **1995**, *67*, 1300-1305.
- [59] Kroon, J. M.; Bakker, N. J.; Smit, H. J. P.; Liska, P.; Thampi, K. R.; Wang, P.; Zakeeruddin, S. M.; Grätzel, M.; Hinsch, A.; Hore, S.; Würfel, U.; Sastrawan, R.; Durrant, J. R.; Palomares, E.; Pettersson, H.; Gruszecki, T.; Walter, J.; Skupien K.; Tulloch, G. E. *Prog. Photovolt.: Res. Appl.* **2007**, *15*, 1-18.
- [60] Ooyama, Y.; Harima, Y. *Eur. J. Org. Chem.* **2009**, 2903-2934.
- [61] Bach, U.; Daeneke, T. *Angew. Chem. Int. Ed.* **2012**, *51*, 10451-10452.

- [62] Galoppini, E. *Coord. Chem. Rev.* **2004**, *248*, 1283-1297.
- [63] Torres, K.; Arrieta, J. P.; Torres, C.; Montero, M L.; Pineda, L. W. *Revista Energía* **2011**, *60*, 6-9.
- [64] Mathew, S.; Yella, A.; Gao, P.; Humphry, R.; Curchod, B. F. E.; Ashari, N.; Tavernelli, I.; Rothlisberger, U.; Nazeeruddin, M. K.; Grätzel, M. *Nat. Chem.* **2014**, *6*, 242-247.
- [65] Wang, C. L.; Hu, J. Y.; Wu, C. H.; Kuo, H. H.; Chang, Y. C.; Lan, Z. J.; Wu, H. P.; Diau, E. W. G.; Lin, C. Y. *Energy Environ. Sci.* **2014**, *7*, 1392-1396.
- [66] Luechai, A.; Pootrakulchote, N.; Kengthanomma, T.; Vanalabhpata, P.; Thamyongkit, P. *J. Organomet. Chem.* **2014**, *753*, 27-33.
- [67] Ikeuchi, T.; Nomoto, H.; Masaki, N.; Griffith, M. J.; Mori, S.; Kimura, M. *Chem. Commun.* **2014**, *50*, 1941-1943.
- [68] Hewat, T. E.; Yellowlees, L. J.; Robertson, N. *Dalton Trans.* **2014**, *43*, 4127-4136.
- [69] Yan, S. G.; Hupp, J. T. *J. Phys. Chem.* **1996**, *100*, 6867-6870.
- [70] Rivera Martínez, M. C., Funcionalización de dióxido de titanio nanoparticulado con diferentes moléculas orgánicas bifuncionales y trímeros de compuestos de transición para la obtención de nuevos materiales, Tesis de Maestría Académica en Química, Universidad de Costa Rica: Ciudad Universitaria Rodrigo Facio, **2012**.
- [71] Camacho, D., Evaluación de varios sustratos modificados de dióxido de titanio (TiO₂) como fotocatalizadores para la producción de hidrógeno a partir de la hidrólisis de agua, Tesis de Licenciatura Ingeniería Química, Universidad de Costa Rica: Ciudad Universitaria Rodrigo Facio, **2012**.
- [72] Joya, K. S.; Joya, Y. F.; Ocakoglu, K.; van de Krol, R. *Angew. Chem. Int. Ed.* **2013**, *52*, 10426-10437.
- [73] Joya, K. S.; Vallés-Pardo, J. L.; Joya, Y. F.; Eisenmayer, T.; Thomas, B.; Buda, F.; de Groot, H. J. M. *ChemPlusChem* **2013**, *78*, 35-47.
- [74] Youngblood, W. J.; Lee, S. H. A.; Maeda, K.; Mallouk, T. E. *Acc. Chem. Res.* **2009**, *42*, 1966-1973.
- [75] Brimblecombe, R.; Koo, A.; Dismukes, G. C.; Swiegers, G. F.; Spiccia, L. *J. Am. Chem. Soc.* **2010**, *132*, 2892-2894.

ACKNOWLEDGEMENTS

The authors are thankful to the Centro de Electroquímica y Energía Química (CELEQ), Universidad de Costa Rica and Vice Presidency of Research, Universidad de Costa Rica (project No. 804-B0-650), Fondo Especial de la Educación Superior (FEES), Consejo Nacional de Rectores (CONARE) and Florida Ice & Farm Co. (Aportes a la Creatividad y la Excelencia) for financial support.